NANO LETTERS

pubs.acs.org/NanoLett Letter

Tiny Clusters for Big Impact in T Cell Activation

Guillaume Le Saux,[#] Piotr Nowakowski,[#] Esti Toledo, Sivan Tzdaka, Shagufta Naaz, Yuval Segal, Brit Maman, Jatin Jawhir Pandit, Muhammed Iraqi, Abed Al-Kader Yassin, Angel Porgador, Ana-Sunčana Smith,* and Mark Schvartzman*

Cite This: *Nano Lett.* 2025, 25, 11878−11887 Read Online

ACCESS | Metrics & More | Article Recommendations | Supporting Information

ABSTRACT: The regulation of T cell activation via engineered arrays holds significant biomedical potential. While average antibody density is known to influence T cell activation, antibody clustering has shown limited benefits. This study challenges this perspective through combined experimental and theoretical approaches. By employing nanolithographically patterned arrays, we show that full T cell activation is achievable with a small number of densely packed antibody clusters—even at average densities where homogeneous or sparsely clustered distributions are insufficient for full activation. These results align with the membrane-fluctuation model that considers cooperative binding and mechanical feedback. Our findings highlight the importance of the spatial organization of activating ligands and provide a framework for designing improved T cell activation platforms for immunotherapy.

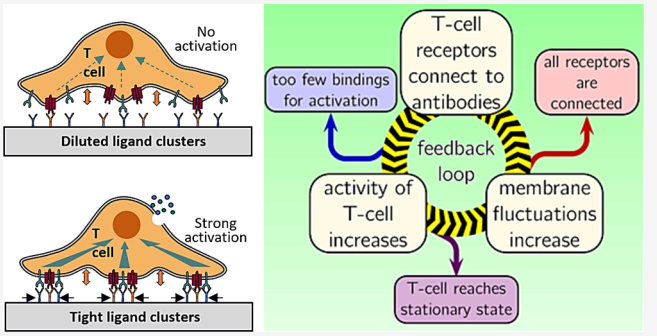

KEYWORDS: *T cell activation, Antibody clustering, Nanolithography, Membrane fluctuation model*

T cells—key players in adaptive immunity—recognize pathogens by binding antigens on cell surfaces via T cell receptors (TCRs). Activation of T cells requires two signals: TCR binding to antigen-MHC complexes on antigen-presenting cells (APCs) and costimulatory binding of CD28 receptor to ligands like B7-1. This triggers a signaling cascade leading to T cell activation, proliferation, differentiation into effector T cells and generation of memory T cells. Understanding T cell activation is crucial not only for the fundamental understanding of T cell immunity but also for advancing new immunotherapies. For example, the generation of chimeric antigen receptor (CAR) T cells[1] requires *ex vivo* T cell activation, which significantly affects the efficiency of CAR transduction and the proliferation of engineered T cells.[2−4]

Ex vivo, T cells are typically activated by stimulating TCR/CD3 and CD28 with antibodies, either in soluble form or bound to artificial antigen-presenting surfaces like plastic microbeads. While both ligand−receptor and antibody−receptor interactions trigger the same signaling pathways, key differences remain; notably, the lower affinity and fast kinetics of ligand−receptor binding enable serial triggering, where one ligand can activate multiple TCRs.[5] High-affinity antibody−receptor binding prevents serial triggering, leading to distinct spatial requirements for T cell activation compared to ligands.[6] Proposed mechanisms of T cell activation are based on: (i) TCR conformation change upon ligand binding,[7] (ii) kinetic segregation,[8,9] where exclusion of large inhibitory phosphatases from tight receptor−ligand region shifts the kinase−phosphatase balance, and (iii) TCR clustering that increases the concentration of signaling molecules.[10,11] These clusters may grow from a few hundred nanometer size in early stages[12,13] to few microns in mature T cell contacts with the target cell.[14−16] The clustering, even at very low ligand concentrations,[17] is promoted by the mobility of ligands and receptors within the cell membrane, optimizing activation.[18] Even so, *ex vivo* activation platforms, like antibody-coated microbeads—the standard in T cell production—use static antibodies, fixing the position of bound receptors.[19−22] Besides the simplicity of production, the preference for *ex vivo* T cell activation platforms with a homogeneous distribution of antibodies stems from the lack of consensus on the role of molecular clustering in T cell activation (reviewed in ref 24).

The pre-existence of nanoscale clusters of TCR in resting T cells, however, remains controversial[23] and the mechanism and role of clustering is still highly debated.[24,25] So far, self-assembled continuous arrays of ligands or antibodies were used to demonstrate the importance of their distribution for activation.[26,27] However, these arrays could not differentiate

Received: April 28, 2025
Revised: July 15, 2025
Accepted: July 15, 2025
Published: July 26, 2025

https://doi.org/10.1021/acs.nanolett.5c02361
Nano Lett. 2025, 25, 11878−11887

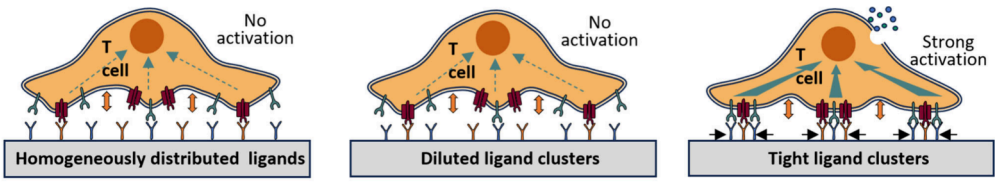

Figure 1. Schematic plot of T cell binding to the substrate with controlled distribution of antibodies. Cell activation is not achieved when antibodies are homogeneously distributed (left panel) or grouped into diluted clusters (middle panel) over the surface at low global densities. As presented on the right panel, full T cell activation is achieved by binding to the substrate with the density of antibodies that is the same as on left panel, but now antibodies are clustered in very dense small clusters.

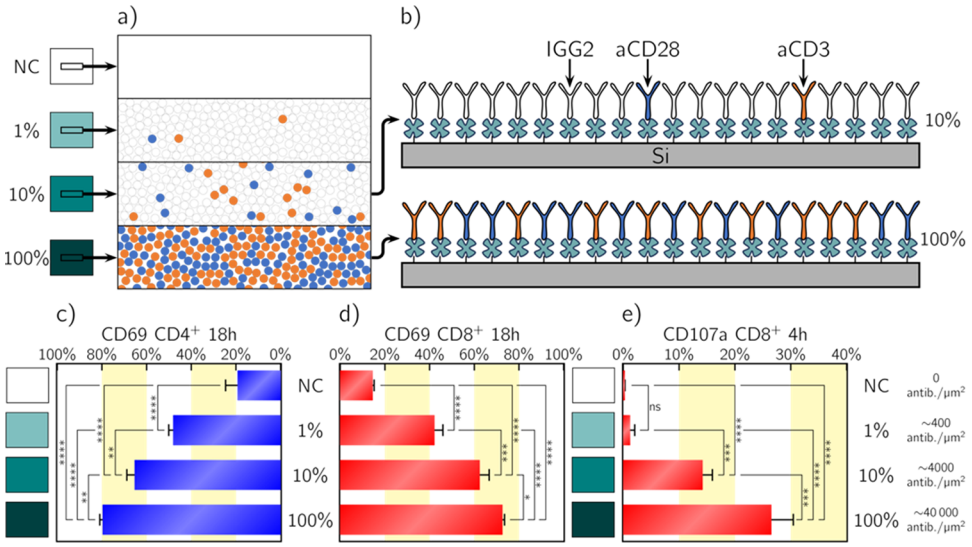

Figure 2. (a) Schematic plot of surface covered with continuous array of antibodies. For 100% continuous array, the surface is fully covered with α-CD3 and α-CD28 antibodies (schematically denoted as orange and blue dots, respectively). For 10% continuous array, only 10% of antibodies are α-CD3/α-CD28. The remaining antibodies are IgG2a isotype controls, which do not bind T cells, schematically denoted with white circles. For 1% continuous array, only 1% of antibodies bind to T cell. Finally, for negative control (NC) there are no antibodies on the substrate. (b) Schematic illustration of the surface covered with antibodies for 10% and 100% continuous arrays. (c) Experimentally measured quantification of CD69 expression for $CD4^+$ cells stimulated on negative control (NC) and continuous arrays (1%, 10%, and 100%) with various dilutions of binding antibodies. (d) Experimentally measured quantification of CD69 expression for $CD8^+$ cells stimulated on negative control and continuous arrays. (e) Experimentally measured quantification of CD107a expression for $CD8^+$ cells stimulated on negative control and continuous arrays. The analysis was performed with Tukey's multiple-comparison tests using the GraphPad Prism software <0.05,**p < 0.01,***p < 0.001,****p < 0.0001.

between the effects of overall density and clustering. Arrays with independently varied clustering and density revealed spatial control of receptor binding but found no impact of TCR clustering on T cell spreading.[23] Importantly, these studies did not assess the effects of antibody/ligand clustering *per se* on T cell response, and focused on activating signaling, neglecting the costimulatory CD28 signaling.

In this work, we focus on understanding the consequences of joint presentation of anti-CD3 and anti-CD28 antibodies in T cell activation, and on resolving the effects of surface density and clustering of these antibodies. We first correlate T cell activation and cytotoxic function with the global density of the two homogeneously distributed proteins and determine the threshold homogeneous density at which T cell activation cannot be determined. Fixed at this global density, we then engineer arrays with antibodies grouped into dense and sparse clusters of varying sizes. This allows us to unambiguously identify the compensatory effects of clustering. Surprisingly, we find that for the same low global density of antibodies, tightly packed small clusters induce full T cell activation, while either homogeneously distributed antibodies or antibodies grouped into differently sized diluted clusters have no effect (Figure 1). These findings are explained by the Membrane Fluctuation Model (MFM) which links antibody−receptor recognition to cellular activity.[28] Our results highlight the critical role of nanoscale antibody clustering in regulating T cell responses, offering insights into immunity and biomaterial design for immunomodulation.

To establish a baseline for studying the effects of antibody density and clustering on T cell activation, we first examined the T cell activation by surfaces coated with homogeneously distributed α-CD3 and α-CD28 at a ratio of 1:1. The surfaces were produced by functionalizing silicon with (3-aminopropyl)tiethoxysilane (APTES), followed by the attachment of polyethylene glycol (PEG)-carboxylic acid terminated with biotin, to which biotinylated antibody mixtures with different dilutions were attached through a neutravidin bridge. Three types of surfaces were used: surfaces with 100% antibody coverage, and surfaces with α-CD3/α-CD28 diluted with human immunoglobulin G2 (IgG2a) at 1:10 and 1:100 ratios. By considering discoid antibody footprint of 5 nm diameter and densely packed antibody arrangement,[29] we

https://doi.org/10.1021/acs.nanolett.5c02361
Nano Lett. 2025, 25, 11878−11887

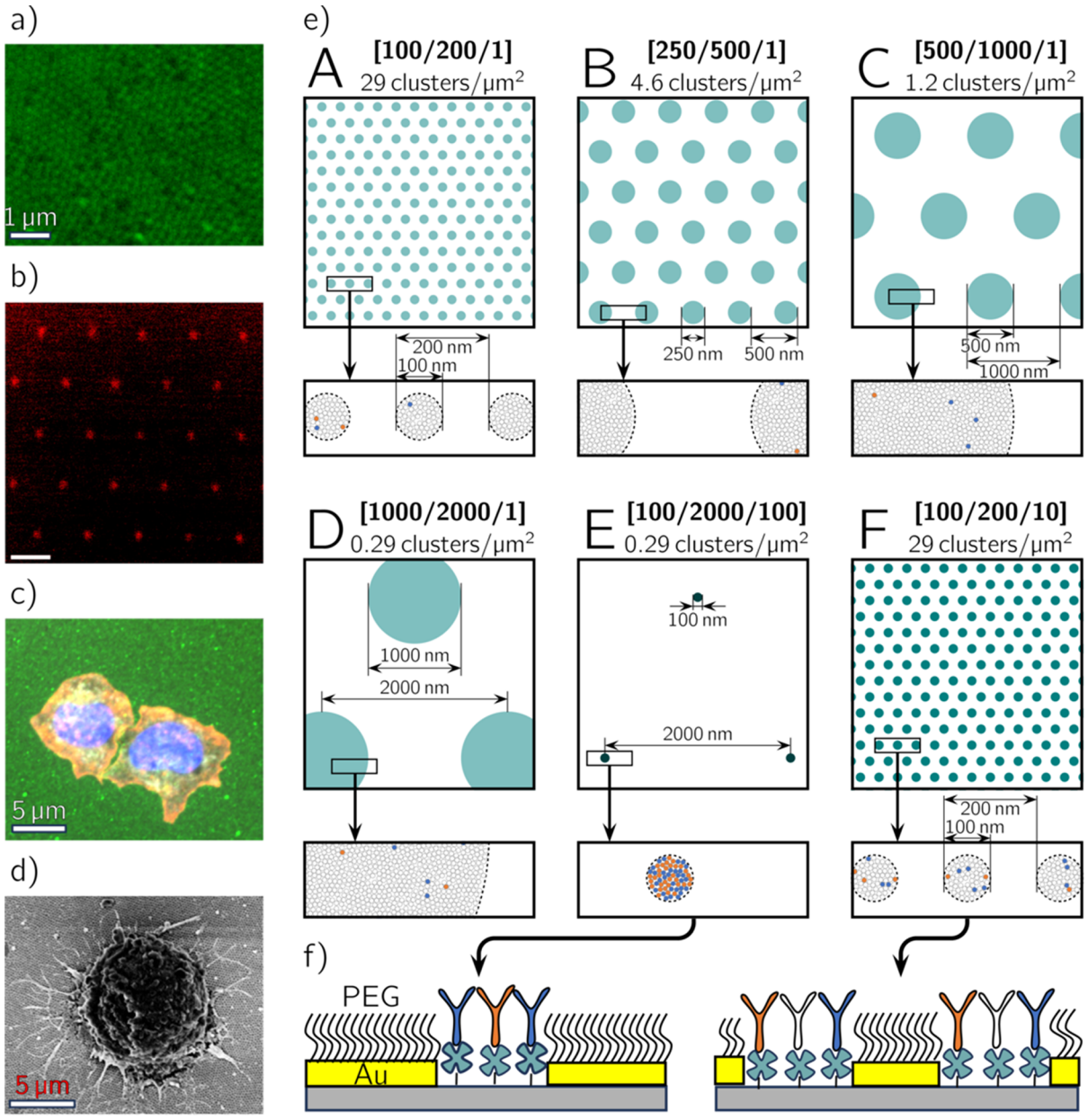

Figure 3. (a) Schematic plots of the patterns used in our study. Each pattern is described with three numbers: distance between neighboring clusters in nm/diameter of each cluster in nm/dilution of the antibodies in percentages. Patterns A, B, C, D, and E have the same overall density of antibodies ~90 μm^{-2}. Pattern F has a density of ~900 μm^{-2}. (b) Schematic plots of the patterned substrates with attached antibodies. (c) High resolution image of clusters of antibodies visualized through the green fluorescently tagged neutravidin. Scale bar: 1 μm. (d) Fluorescent image of 100 nm antibody clusters separated by 2 μm. Scale bar: 2 μm. (e) Fluorescent microscopy of T cells spread on an array of antibody clusters. Avidin used for binding the antibodies to silicon surfaces was tagged with green, and the cells were tagged with red phalloidin for cytoskeleton and blue DAPI for nucleus. Scale bar: 5 μm. (f) Scanning electron micrograph of T cell spread on the nanoarray. Scale bar: 5 μm.

estimate that this produced global α-CD3 and α-CD28 densities of ~400, ~4000, and ~40,000 antibodies/μm^2 (Figure 2a,b).

Peripheral Blood Mononuclear Cells (PBMCs) from a healthy donor were used as a source of T cells. The PBMCs were seeded onto patterned surfaces in 96-well plates, stimulated, and then stained for CD3, CD4, CD8, for flow cytometry analysis. The activation was assessed by flow cytometry using two markers: CD69 after 18 h of stimulation, and CD107a (degranulation marker) after 4 h of stimulation. As expected, the lowest α-CD3 and α-CD28 density produced only ~40% CD69-positive cells, compared to ~80% for surfaces at full α-CD3 and α-CD28 coverage. CD107a expression in $CD8^+$ cells was only ~2% at the lowest density versus ~25% at the highest, with negligible degranulation in $CD4^+$ T cells due to their noncytotoxic nature. This suggests that our lowest homogeneous density is insufficient to fully activate T cells. However, the activation gradually increases with density until fully activated cells are observed at surfaces continuously covered by antibodies, consistently with activation observed using only α-CD3.[20] Also, similar trend of activation vs antibody density was observed using IFN-γ assessed by ELISA after 18 h of activation, although with less

https://doi.org/10.1021/acs.nanolett.5c02361
Nano Lett. 2025, 25, 11878−11887

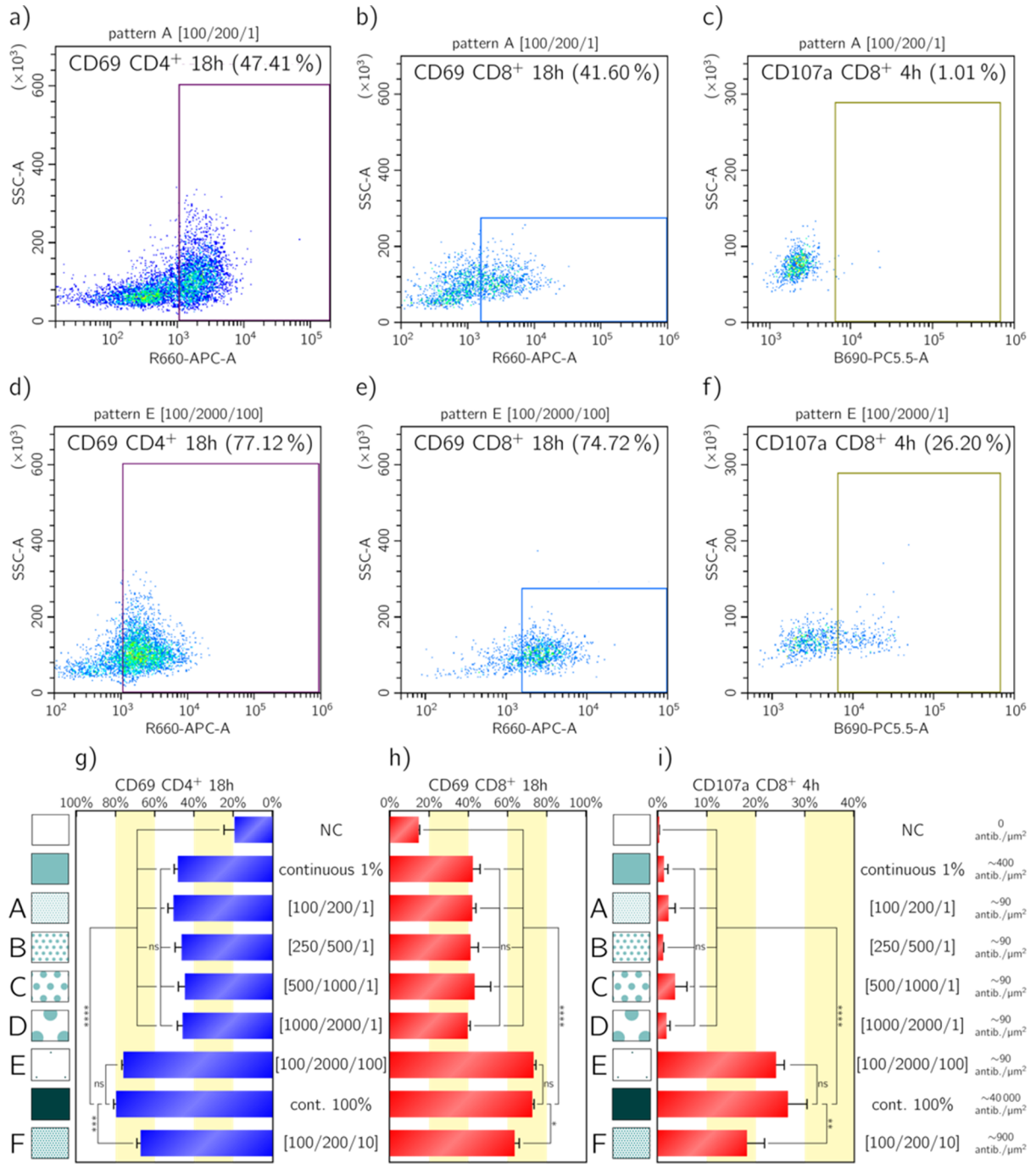

Figure 4. CD4+ and CD8+ activation on different patterned substrates. (a)−(f) Representative examples of flow cytometry measurements for CD69 (a, b) and CD107a (c−f) expression for patterns A [100/200/1] (a,c,e) and E [100/2000/100] (b, d, f). Experimentally measured quantification of CD69 expression for CD4+ (g) and CD8+ (h) cells stimulated on various patterned substrates. (i) Expression of CD107a for CD8+ cells stimulated on various patterned substrates. The analysis was performed with Tukey's multiple-comparison tests using the GraphPad Prism software <0.05,**p < 0.01,***p < 0.001,****p < 0.0001.

pronounced differences between various densities, likely to the contributions of other cells presenting in PBMCs (Figure S1).

Following this initial observation, we selected the 1:100 (α-CD3/α-CD28):IgG2a dilution as a benchmark for full T cell activation, to examine the potentially compensatory effect of antibody clustering. To that end, we designed a series of arrays of disk-shaped antibody clusters, maintaining the 1:100 (α-CD3/α-CD28):IgG2a dilution within each disk. Disk sizes ranged from 100 nm to 1 μm, with center-to-center spacing set at twice the disks diameter (Figure 3a, patterns A−D). In all these configurations, despite different sizes and separations, disks, and therefore the antibody clusters occupied approximately 23% of the total surface area, resulting in a theoretical global α-CD3/α-CD28 density of ~90 antibodies/μm^2.

These arrays (A−D) were created using nanosphere lithography, an ideal method for producing dense nanoscale patterns.[30] Polystyrene nanospheres were assembled into a closely packed hexagonal monolayer on a silicon surface, using either the Langmuir−Blodgett method for 200 nm spheres or a dry method for larger spheres.[31] The spheres were etched by

https://doi.org/10.1021/acs.nanolett.5c02361
Nano Lett. 2025, 25, 11878−11887

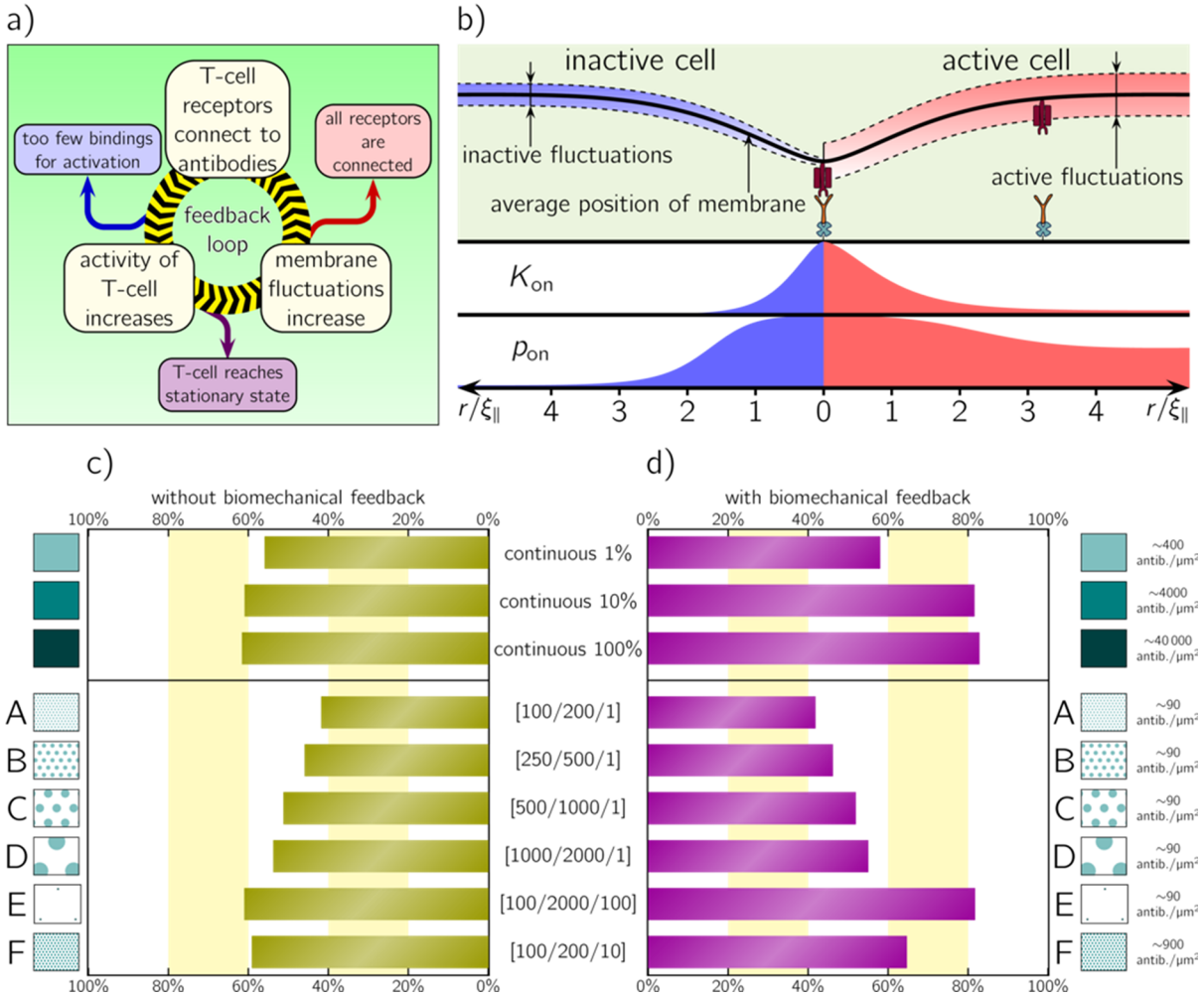

Figure 5. (a) Schematic plot of the biomechanical feedback loop in Membrane Fluctuation Model. Binding of receptors on the membrane of T cell is increasing activity of the cell, and as a result, membrane fluctuations are increasing which promotes further binding. (b) Schematic comparison of the binding process for inactive (left side) and active cell (right side). For active cell the fluctuations of the membrane are stronger (as illustrated in top part of the scheme). As a result, both binding rate K_{on} and probability p_{on} of binding of next receptor is increased. (c) Numerical simulations of activity of cell assuming there is no biomechanical feedback (and thus only inactive fluctuations are present) for continuous arrays (top part) and for all the patterns presented in Figure 3a. (d) The same results as on panel (c) but with the mechanism of biomechanical feedback increasing the cell membrane fluctuations.

oxygen plasma to halve their diameter, followed by gold evaporation in the interstices of the nanosphere array Nanosphere lift-off created a hexagonal array of silicon discs surrounded by a gold background (Figure S2). This results in a set of patterns which we denominate with three indices [disk diameter in nm/disk periodicity in nm/percentage of α-CD3/α-CD28 in the antibody mix within the disk]. As shown in Figure 3a, pattern A, noted [100/200/1] yields 29 disks /μm^2, pattern B [250/500/1] 4.6 disks/μm^2, pattern C [500/1000/1] 1.2 disks/μm^2, and pattern D [1000/2000/1] 0.29 disk/μm^2. These designs allow us to assess if the introduction of a particular length scale in the antibody organization affects T cell activation.

Also, to investigate the role of local antibody density within clusters, we designed a pattern of disks as small as in pattern A (100 nm) but separated by 2 μm (Figure 3a, pattern E, and Figure S3). In these 100 nm disks, the antibodies were not diluted, i.e. contained 100% α-CD3/α-CD28, and thus mimicked the dimensions of receptor clusters in resting T cells.[25] For pattern E [100/2000/100], the 10-fold larger distance between the clusters was designed to keep the global density of ~90 antibodies/μm^2 as in patterns A–D. This pattern, denominated as pattern E [100/2000/100] with 0.29 disks /μm^2, was produced by electron-beam lithography of negative tone resist, which was followed by gold evaporation and liftoff. Notably, a T cell with a typical spreading area of 5–10 μm^2 can be exposed only to one or two such clusters on average.

Finally, along the same line of thought that the density of proteins within clusters and not the cluster size itself or the number of clusters affects activation, we prepared a pattern with a geometry identical to that of cluster A, but increased the concentration of α-CD3/α-CD28 to 10% by 1:10 (α-CD3/α-CD28):IgG2a dilution (pattern F [100/200/10], achieving an average density of ~900 antibodies/μm^2 and 29 disks/μm^2). All patterns, regardless of their fabrication methods, were functionalized by various mixtures of α-CD3/α-CD28 and IgG2a, which were linked to oxidized silicon nanodiscs via APTES, PEG, and biotin chemistries. The surrounding gold was passivated by PEG to prevent nonspecific binding. Biofunctionalization specificity was confirmed by confocal microscopy (Figure 3c,d).

https://doi.org/10.1021/acs.nanolett.5c02361
Nano Lett. 2025, 25, 11878–11887

We then studied T cell activation on surfaces with coclustered α-CD3 α-CD28. As in baseline experiments, PBMCs from a healthy donor were plated on antibody-patterned surfaces, fixed, and stained for cytoskeletal and nuclear markers (Figure 3e). Fluorescence and electron microscopy confirmed T cell spreading, tight contact with clusters, and formation of nanometric protrusions resembling microvilli.[32,33] Activation was assessed by CD69 (18 h) and CD107a (4 h) expression via flow cytometry (Figure 4a–f), with PEG-coated gold as a negative control. Patterns A–D, despite presenting many 100 nm clusters, showed minimal CD69 expression—similar to low-density continuous coatings—indicating no clustering compensation at this global density. In contrast, pattern E, featuring small, widely spaced but tightly packed clusters, significantly increased CD69 expression in both $CD4^+$ and $CD8^+$ cells (Figure 4g, h), outperforming even pattern F, which had 10-fold higher antibody density. In fact, pattern E's activation level approached that of densely coated homogeneous surfaces.

The interplay between global α-CD3/α-CD28 density and clustering is even more pronounced when examining CD107a. The difference between the A–D and E configurations resulted in more than a 10-fold increase in the percentage of $CD8^+$ cells expressing CD107a (Figure 4i), providing a level of activation larger than pattern F, and not showing significant differences to a continuous, fully packed surface. This demonstrates that while a low global antibody density may be insufficient for full T cell activation when antibodies are randomly distributed, confining them into dense clusters can compensate for this limitation. Furthermore, this shows that the size of the cluster is not definitive for T cell activation but that it is enough to create a small number of stable bindings.

It is noteworthy that here, as in our previous work,[34] we used PBMCs, which, in addition to primary T cells, also contain various amounts of NK cells, APCs and B cells. However, both our continuous array and patterned surfaces were coated with α-CD3/α-CD28, and were therefore T cell-specific, thus ensuring a minimal effect of these surfaces on other cell types present in the PBMC population. This, in turn, ensured a minimal impact of other cell types on T cells across different used activation surfaces. This is confirmed by the consistently significant differences in CD69 and CD107a levels between surfaces with and without α-CD3/α-CD28, thus ensuring the negligible effect of other cell types on the CD69 and CD107a signals produced by T cells.

These observations can be rationalized by adapting the so-called Membrane Fluctuation Model (MFM) for immune cell activation (Figure 5a) originally conceived for natural killer cells.[28,35] In essence, MFM captures the dynamic coupling between the ligand–receptor binding and the activity of the cell through a mechanical feedback (Figure 5b), while the rates for binding and unbinding directly depend on the proximity of neighboring ligand(antibody)–receptor constructs. The model assumes that the activation is proportional to the density $\mathcal{N}$ of ligand–receptor bonds of the cell, which, in the stationary state, is given by $\mathcal{N} = \varrho\overline{K_{on}}/(\overline{K_{off}} + \overline{K_{on}})$, with ϱ denoting antibody density, and $\overline{K_{on}}$ and $\overline{K_{off}}$ being average binding and unbinding rates, respectively. These average rates are calculated from the first-principles assuming bonds to be springs with defined stiffness and rest length (see SI for details), while the averaging is performed over possible surface binding sites and bond distributions.[36]

MFM was first applied to homogeneous antibody distributions, showing that T cell signaling increases with global antibody density (Figure 5c, d, top). However, only when mechanical feedback was included—linking cell activity to the fraction of bound antibodies rather than average density—did the model align qualitatively with experimental results (see SI for a more detailed discussion). The lowest probed density of ~400 antibodies/μm^2 produced the lowest percentage of bounded receptors, which initiated partial biomechanical feedback and could not induce full activation. Yet, the activity of the cell increases between ~400 and ~4000 antibodies/μm^2, until it reaches saturation between ~4000 and 40,000 antibodies/μm^2. This highlights the fact that activation is indeed a process in which the dynamic evolution of the number of formed bonds influences the state of the cell and consequently, the state of the membrane. We, furthermore, conclude that undiluted arrays provide an excess amount of activating and costimulatory signal.[37]

Encouraged by this agreement, we applied the MFM model to patterned surfaces (Figure 5c, d, bottom). As in experiments, diluted patterns failed to trigger mechanical feedback, while dense clustering of antibodies—even at low global densities—enhanced binding rates and bond stability, activating T cells through a proximity-driven feedback loop (Figure 5b). MFM shows that the binding and unbinding rates (K_{on}, K_{off} respectively) are directly coupled to the membrane configuration and are explicit functions of the average height and the fluctuation amplitude, while the latter increases with the cell activity following a logistic function.[39] Following previous arguments, TCR receptor binding induces transversal proximity between the T cell and a target cell, but away from the bond, the gap between the two membranes is set by the size of large phosphatase molecules.[38–40] This is directly implemented in the MFM model by setting the size of the ligand–receptor bond and the parametrization of the gap. MFM model shows that both the deformation of the membrane due to antibody binding and the change of fluctuations due to change in activity is necessary to initiate biomechanical feedback.

The result is strongly increased binding close to an existing bond in a transversal proximity of about 40 nm[41,42] due to the finite lateral correlation length of the membrane.[43] This further facilitates the formation of more similarly sized ligand–receptor bonds around already formed bonds.[44] The accumulation of these bonds can counteract the repulsive forces between the membranes, further stabilizing the bonds, even in an activated state.[45] The formation of bonds triggers the signaling and initiates the activation process, which, in turn, changes the state of the cell, enhancing the cytoskeleton dynamics, cytoplasmic flows and/or ion channel activity among other processes. The ensemble of these processes boosts the dynamics of the membrane, which is reflected in increasing fluctuation amplitudes with activation.[25,39] In turn, a change in membrane fluctuations leads to changes in the binding and unbinding rates, hence serving as mechanical feedback. Nearby receptors on the membrane are affected in a geometry-dependent manner, yielding strong correlations that promote further binding. Hence, the amplification process ensues until the number of bonds and the activity of the cell saturates in a new steady state. Therefore, even though a certain global antibody density could be insufficient for full T cell activation if the antibodies are randomly distributed over the surface, a compensatory effect can be achieved at the same

https://doi.org/10.1021/acs.nanolett.5c02361
Nano Lett. 2025, 25, 11878–11887

density if the antibodies are grouped into clusters. Interestingly, these small cluster sizes and large periodicity mimic the ligand−receptor nanoclusters observed at the physiological interface between T cells and target cells.[46]

In summary, our study demonstrates that clustering plays a central role in regulating T cell activation, particularly at low ligand or antibody densities—a finding well accounted for by the membrane fluctuation model. This model highlights membrane elasticity as a key contributor to the clustering mechanism while integrating the well-established increase in cytoskeletal dynamics in activation. The resulting rapid actin remodeling, cytoplasmic flows, and enhanced membrane trafficking significantly modulate membrane fluctuations, owing to the membrane's low bending stiffness. A critical next step will be to directly correlate T cell binding dynamics with quantitative measurements of membrane state. Experimentally, this could be done, for instance, by combining dynamic optical displacement spectroscopy with super-resolution microscopy, alongside precise control of photobleaching. An alternative approach could involve reflection interference contrast microscopy operated in dynamic fluctuation mode; however, without accounting for the evolution of the refractive index, this method would only provide relative amplitude measurements. Although such simultaneous measurements present substantial technical challenges, they remain a crucial objective for future work, as they would provide definitive evidence of the role of cell mechanics in T cell activation.

Additional research should, furthermore, combine clustering with additional mechanical cues, such as the viscoelasticity[47−50] and nanoscale topography[51−54] of the surface to which the molecules are tethered. This is possible by using reductionist platforms that controllably alter each of these parameters[55] while combining them with patterning methods,[26,56−59] which today are achieving control at the individual molecule level.[60−62] Such sophisticated platforms will offer valuable insights into the forces exerted by cells and their correlation with immune responses. This will lay the foundation for optimizing mechanical stimuli and drive significant progress in understanding the physical mechanisms underlying T cell activation.

We believe that, beyond providing insights into the fundamental mechanisms of T cell activation, our findings pave the way for the development of next-generation T cell priming platforms for clinical applications, such as adoptive T cell transfer and Chimeric Antigen Receptor (CAR) T cell immunotherapy. Current T cell priming approaches—such as those based on beads coated with activating and costimulatory antibodies—deliver a maximal dose of stimulation due to the uncontrolled and dense distribution of surface-bound antibodies. However, it is increasingly evident that excessive stimulation does not necessarily yield optimal antitumor potency,[63] as overstimulation can lead to rapid T cell exhaustion. By further exploring the strategy of tuning activation through antibody clustering, one could design immunotherapeutic priming platforms in which activating and costimulatory molecules (e.g., receptor-specific ligands or antibodies) are presented in well-defined nanoclusters with controlled size and spacing. According to our findings, this approach could maintain an overall low stimulus level per T cell while still enabling adequate activation—sufficient for effective transfection with artificial receptors and for expansion to clinically relevant cell numbers—while minimizing exhaustion and prolonging antitumor effects.

Finally, T cell priming platforms could harness this newly generated understanding of the importance of molecular clustering in synergy with other mechanical stimuli. We have already demonstrated that tuning the microtopography and elasticity of the surface enables the production of CAR T cells with antitumor potency exceeding that of T cells generated by standard priming methods, even with excessive concentrations of tethered antibodies.[64] Moving forward, engineering an optimized T cell priming platform, where all physical parameters are precisely orchestrated, offers a promising path toward achieving superior immunotherapeutic outcomes.

■ ASSOCIATED CONTENT

Data Availability Statement

Associated content: The raw data is available at Zenodo DOI: 10.5281/zenodo.15546431.

Supporting Information

The Supporting Information is available free of charge at https://pubs.acs.org/doi/10.1021/acs.nanolett.5c02361.

Materials and methods; flow cytometry data with statistics, showing the impact of antibody surface density on IFNγ, CD69, and CD107a expressions; SEM analyses of the nanoarrays, and further explaination of the Membrane Fluctuation Model (PDF)

■ AUTHOR INFORMATION

Corresponding Authors

Ana-Sunčana Smith − *Group for Computational Life Sciences, Division of Physical Chemistry, Ruđer Bošković Institute, 10000 Zagreb, Croatia; PULS Group, Institut für Theoretische Physik, IZNF, Friedrich-Alexander-Universität Erlangen-Nürnberg, 91058 Erlangen, Germany;* orcid.org/0000-0002-0835-0086; Email: smith@physik.fau.de, asmith@irb.hr

Mark Schvartzman − *Department of Materials Engineering, Faculty of Engineering, Ben-Gurion University of the Negev, Beer-Sheva 84105, Israel; Ilse Katz Institute for Nanoscale Science and Technology, Ben-Gurion University of the Negev, Beer-Sheva 84105, Israel;* orcid.org/0000-0002-5912-525X; Email: marksc@bgu.ac.il

Authors

Guillaume Le Saux − *Department of Materials Engineering, Faculty of Engineering, Ben-Gurion University of the Negev, Beer-Sheva 84105, Israel; Ilse Katz Institute for Nanoscale Science and Technology, Ben-Gurion University of the Negev, Beer-Sheva 84105, Israel*

Piotr Nowakowski − *Group for Computational Life Sciences, Division of Physical Chemistry, Ruđer Bošković Institute, 10000 Zagreb, Croatia;* orcid.org/0000-0001-6169-2416

Esti Toledo − *Department of Materials Engineering, Faculty of Engineering, Ben-Gurion University of the Negev, Beer-Sheva 84105, Israel; Ilse Katz Institute for Nanoscale Science and Technology, Ben-Gurion University of the Negev, Beer-Sheva 84105, Israel;* orcid.org/0000-0003-3103-816X

Sivan Tzdaka − *Department of Materials Engineering, Faculty of Engineering, Ben-Gurion University of the Negev, Beer-Sheva 84105, Israel; Ilse Katz Institute for Nanoscale Science*

and Technology, Ben-Gurion University of the Negev, Beer-Sheva 84105, Israel

Shagufta Naaz − *Department of Materials Engineering, Faculty of Engineering, Ben-Gurion University of the Negev, Beer-Sheva 84105, Israel; Ilse Katz Institute for Nanoscale Science and Technology, Ben-Gurion University of the Negev, Beer-Sheva 84105, Israel*

Yuval Segal − *Department of Materials Engineering, Faculty of Engineering, Ben-Gurion University of the Negev, Beer-Sheva 84105, Israel; Ilse Katz Institute for Nanoscale Science and Technology, Ben-Gurion University of the Negev, Beer-Sheva 84105, Israel*

Brit Maman − *Department of Materials Engineering, Faculty of Engineering, Ben-Gurion University of the Negev, Beer-Sheva 84105, Israel; Ilse Katz Institute for Nanoscale Science and Technology, Ben-Gurion University of the Negev, Beer-Sheva 84105, Israel*

Jatin Jawhir Pandit − *Department of Materials Engineering, Faculty of Engineering, Ben-Gurion University of the Negev, Beer-Sheva 84105, Israel; Ilse Katz Institute for Nanoscale Science and Technology, Ben-Gurion University of the Negev, Beer-Sheva 84105, Israel*

Muhammed Iraqi − *Department of Microbiology and Immunology, and Genetics, Faculty of Health Sciences, Ben-Gurion University of the Negev, Beer-Sheva 84105, Israel*

Abed Al-Kader Yassin − *Department of Microbiology and Immunology, and Genetics, Faculty of Health Sciences, Ben-Gurion University of the Negev, Beer-Sheva 84105, Israel*

Angel Porgador − *Department of Microbiology and Immunology, and Genetics, Faculty of Health Sciences, Ben-Gurion University of the Negev, Beer-Sheva 84105, Israel*

Complete contact information is available at: https://pubs.acs.org/10.1021/acs.nanolett.5c02361

Author Contributions

#Guillaume Le Saux and Piotr Nowakowski contributed equally.

Notes

The authors declare no competing financial interest.

■ ACKNOWLEDGMENTS

A.-S.S. and M.S. gratefully acknowledge the support of the German Research Foundation via Joint Project SM 289/10-1. M.S. acknowledges the support of the Israel Science Foundation Project 2016/21. A.-S.S. and P.N. received further support by the German Science Foundation and the French National Research Agency Project SM 289/8-1.

■ REFERENCES

(1) Long, A. H.; Haso, W. M.; Shern, J. F.; Wanhainen, K. M.; Murgai, M.; Ingaramo, M.; Smith, J. P.; Walker, A. J.; Kohler, M. E.; Venkateshwara, V. R.; Kaplan, R. N.; Patterson, G. H.; Fry, T. J.; Orentas, R. J.; Mackall, C. L. 4−1BB Costimulation Ameliorates T Cell Exhaustion Induced by Tonic Signaling of Chimeric Antigen Receptors. *Nat. Med.* **2015**, *21* (6), 581−590.

(2) Waldman, A. D.; Fritz, J. M.; Lenardo, M. J. A Guide to Cancer Immunotherapy: From T Cell Basic Science to Clinical Practice. *Nat. Rev. Immunol.* **2020**, *20* (11), 651−668.

(3) Li, R.; Ma, C.; Cai, H.; Chen, W. The CAR T-Cell Mechanoimmunology at a Glance. *Adv. Sci.* **2020**, *7* (24), 2002628.

(4) Zhang, D. K. Y.; Adu-Berchie, K.; Iyer, S.; Liu, Y.; Cieri, N.; Brockman, J. M.; Neuberg, D.; Wu, C. J.; Mooney, D. J. Enhancing CAR-T Cell Functionality in a Patient-Specific Manner. *Nat. Commun.* **2023**, *14* (1), 506.

(5) Huang, J.; Zarnitsyna, V. I.; Liu, B.; Edwards, L. J.; Jiang, N.; Evavold, B. D.; Zhu, C. The Kinetics of Two-Dimensional TCR and pMHC Interactions Determine T-Cell Responsiveness. *Nature* **2010**, *464* (7290), 932−936.

(6) Hellmeier, J.; Platzer, R.; Eklund, A. S.; Schlichthaerle, T.; Karner, A.; Motsch, V.; Schneider, M. C.; Kurz, E.; Bamieh, V.; Brameshuber, M.; Preiner, J.; Jungmann, R.; Stockinger, H.; Schütz, G. J.; Huppa, J. B.; Sevcsik, E. DNA Origami Demonstrate the Unique Stimulatory Power of Single pMHCs as T Cell Antigens. *Proc. Natl. Acad. Sci. U. S. A.* **2021**, *118* (4), No. e2016857118.

(7) Minguet, S.; Swamy, M.; Alarcón, B.; Luescher, I. F.; Schamel, W. W. A. Full Activation of the T Cell Receptor Requires Both Clustering and Conformational Changes at CD3. *Immunity* **2007**, *26* (1), 43−54.

(8) Davis, S. J.; van der Merwe, P. A. The Kinetic-Segregation Model: TCR Triggering and Beyond. *Nat. Immunol.* **2006**, *7* (8), 803−809.

(9) Choudhuri, K.; Wiseman, D.; Brown, M. H.; Gould, K.; Van Der Merwe, P. A. T-Cell Receptor Triggering Is Critically Dependent on the Dimensions of Its Peptide-MHC Ligand. *Nature* **2005**, *436* (7050), 578−582.

(10) Kumari, S.; Curado, S.; Mayya, V.; Dustin, M. L. T Cell Antigen Receptor Activation and Actin Cytoskeleton Remodeling. *Biochim. Biophys. Acta BBA - Biomembr.* **2014**, *1838* (2), 546−556.

(11) Krogsgaard, M.; Davis, M. M. How T Cells "see" Antigen. *Nat. Immunol.* **2005**, *6* (3), 239−245.

(12) Roh, K.-H.; Lillemeier, B. F.; Wang, F.; Davis, M. M. The Coreceptor CD4 Is Expressed in Distinct Nanoclusters and Does Not Colocalize with T-Cell Receptor and Active Protein Tyrosine Kinase P56lck. *Proc. Natl. Acad. Sci. U. S. A.* **2015**, *112* (13), E1604−E1613.

(13) Pageon, S. V.; Tabarin, T.; Yamamoto, Y.; Ma, Y.; Nicovich, P. R.; Bridgeman, J. S.; Cohnen, A.; Benzing, C.; Gao, Y.; Crowther, M. D.; Tungatt, K.; Dolton, G.; Sewell, A. K.; Price, D. A.; Acuto, O.; Parton, R. G.; Gooding, J. J.; Rossy, J.; Rossjohn, J.; Gaus, K. Functional Role of T-Cell Receptor Nanoclusters in Signal Initiation and Antigen Discrimination. *Proc. Natl. Acad. Sci. U. S. A.* **2016**, *113* (37), E5454−E5463.

(14) Yokosuka, T.; Saito, T. Dynamic Regulation of T-Cell Costimulation through TCR-CD28 Microclusters. *Immunol. Rev.* **2009**, *229* (1), 27−40.

(15) Varma, R.; Campi, G.; Yokosuka, T.; Saito, T.; Dustin, M. L. T Cell Receptor-Proximal Signals Are Sustained in Peripheral Microclusters and Terminated in the Central Supramolecular Activation Cluster. *Immunity* **2006**, *25* (1), 117−127.

(16) Schamel, W. W. A.; Alarcón, B. Organization of the Resting TCR in Nanoscale Oligomers. *Immunol. Rev.* **2013**, *251* (1), 13−20.

(17) Smith, A.-S.; Sengupta, K.; Goennenwein, S.; Seifert, U.; Sackmann, E. Force-Induced Growth of Adhesion Domains Is Controlled by Receptor Mobility. *Proc. Natl. Acad. Sci. U. S. A.* **2008**, *105* (19), 6906−6911.

(18) Dillard, P.; Varma, R.; Sengupta, K.; Limozin, L. Ligand-Mediated Friction Determines Morphodynamics of Spreading T Cells. *Biophys. J.* **2014**, *107*, 2629−2638.

(19) Adu-Berchie, K.; Mooney, D. J. Biomaterials as Local Niches for Immunomodulation. *Acc. Chem. Res.* **2020**, *53* (9), 1749−1760.

(20) Cheung, A. S.; Zhang, D. K. Y.; Koshy, S. T.; Mooney, D. J. Scaffolds That Mimic Antigen-Presenting Cells Enable Ex Vivo Expansion of Primary T Cells. *Nat. Biotechnol.* **2018**, *36* (2), 160−169.

(21) Schluck, M.; Hammink, R.; Figdor, C. G.; Verdoes, M.; Weiden, J. Biomaterial-Based Activation and Expansion of Tumor-Specific T Cells. *Front. Immunol.* **2019**, *10*, 931.

(22) Han, B.; Song, Y.; Park, J.; Doh, J. Nanomaterials to Improve Cancer Immunotherapy Based on Ex Vivo Engineered T Cells and NK Cells. *J. Control. Release Off. J. Control. Release Soc.* **2022**, *343*, 379−391.

(23) Rossboth, B.; Arnold, A. M.; Ta, H.; Platzer, R.; Kellner, F.; Huppa, J. B.; Brameshuber, M.; Baumgart, F.; Schütz, G. J. TCRs Are Randomly Distributed on the Plasma Membrane of Resting Antigen-Experienced T Cells. *Nat. Immunol.* **2018**, *19* (8), 821−827.
(24) Sengupta, K.; Dillard, P.; Limozin, L. Morphodynamics of T-Lymphocytes: Scanning to Spreading. *Biophys. J.* **2024**, *123*, 2224.
(25) Goyette, J.; Nieves, D. J.; Ma, Y.; Gaus, K. How Does T Cell Receptor Clustering Impact on Signal Transduction? *J. Cell Sci.* **2019**, *132* (4), No. jcs226423.
(26) Matic, J.; Deeg, J.; Scheffold, A.; Goldstein, I.; Spatz, J. P. Fine Tuning and Efficient T Cell Activation with Stimulatory aCD3 Nanoarrays. *Nano Lett.* **2013**, *13* (11), 5090−5097.
(27) Delcassian, D.; Depoil, D.; Rudnicka, D.; Liu, M.; Davis, D. M.; Dustin, M. L.; Dunlop, I. E. Nanoscale Ligand Spacing Influences Receptor Triggering in T Cells and NK Cells. *Nano Lett.* **2013**, *13* (11), 5608−5614.
(28) Pandey, A.; Nowakowski, P.; Ureña Martin, C.; Abu Ahmad, M.; Edri, A.; Toledo, E.; Tzadka, S.; Walther, J.; Le Saux, G.; Porgador, A.; Smith, A.-S.; Schvartzman, M. Membrane Fluctuation Model for Understanding the Effect of Receptor Nanoclustering on the Activation of Natural Killer Cells through Biomechanical Feedback. *Nano Lett.* **2024**, *24* (18), 5395−5402.
(29) Hinrichsen, E. L.; Feder, J.; Jøssang, T. Random Packing of Disks in Two Dimensions. *Phys. Rev. A* **1990**, *41* (8), 4199−4209.
(30) Agheli, H.; Malmström, J.; Larsson, E. M.; Textor, M.; Sutherland, D. S. Large Area Protein Nanopatterning for Biological Applications. *Nano Lett.* **2006**, *6* (6), 1165−1171.
(31) Tzadka, S.; Ureña Martin, C.; Toledo, E.; Yassin, A. A. K.; Pandey, A.; Le Saux, G.; Porgador, A.; Schvartzman, M. A Novel Approach for Colloidal Lithography: From Dry Particle Assembly to High-Throughput Nanofabrication. *ACS Appl. Mater. Interfaces* **2024**, *16* (14), 17846−17856.
(32) Jung, Y.; Riven, I.; Feigelson, S. W.; Kartvelishvily, E.; Tohya, K.; Miyasaka, M.; Alon, R.; Haran, G. Three-Dimensional Localization of T-Cell Receptors in Relation to Microvilli Using a Combination of Superresolution Microscopies. *Proc. Natl. Acad. Sci. U. S. A.* **2016**, *113* (40), E5916−E5924.
(33) Razvag, Y.; Neve-Oz, Y.; Sajman, J.; Reches, M.; Sherman, E. Nanoscale Kinetic Segregation of TCR and CD45 in Engaged Microvilli Facilitates Early T Cell Activation. *Nat. Commun.* **2018**, *9* (1), 732.
(34) Pandit, J. J.; Yassin, A. A.-K.; Martin, C. U.; Saux, G. L.; Porgador, A.; Schvartzman, M. Effect of Binary Mechanical Environment on T Cell Function. *Acta Biomater.* **2025**, *195*, 83−93.
(35) Toledo, E.; Le Saux, G.; Edri, A.; Li, L.; Rosenberg, M.; Keidar, Y.; Bhingardive, V.; Radinsky, O.; Hadad, U.; Di Primo, C.; Buffeteau, T.; Smith, A.-S.; Porgador, A.; Schvartzman, M. Molecular-Scale Spatio-Chemical Control of the Activating-Inhibitory Signal Integration in NK Cells. *Sci. Adv.* **2021**, *7* (24), No. eabc1640.
(36) Janeš, J. A.; Monzel, C.; Schmidt, D.; Merkel, R.; Seifert, U.; Sengupta, K.; Smith, A.-S. First-Principle Coarse-Graining Framework for Scale-Free Bell-Like Association and Dissociation Rates in Thermal and Active Systems. *Phys. Rev. X* **2022**, *12* (3), No. 031030.
(37) Schodin, B. A.; Tsomides, T. J.; Kranz, D. M. Correlation Between the Number of T Cell Receptors Required for T Cell Activation and TCR−Ligand Affinity. *Immunity* **1996**, *5* (2), 137−146.
(38) Bruinsma, R.; Behrisch, A.; Sackmann, E. Adhesive Switching of Membranes: Experiment and Theory. *Phys. Rev. E Stat. Phys. Plasmas Fluids Relat. Interdiscip. Top.* **2000**, *61* (4), 4253−4267.
(39) Sackmann, E.; Smith, A.-S. Physics of Cell Adhesion: Some Lessons from Cell-Mimetic Systems. *Soft Matter* **2014**, *10* (11), 1644−1659.
(40) Weikl, T. R.; Lipowsky, R. Pattern Formation during T-Cell Adhesion. *Biophys. J.* **2004**, *87* (6), 3665−3678.
(41) Allard, J. F.; Dushek, O.; Coombs, D.; van der Merwe, P.A. Mechanical Modulation of Receptor-Ligand Interactions at Cell-Cell Interfaces. *Biophys. J.* **2012**, *102* (6), 1265−1273.
(42) Dushek, O.; Goyette, J.; van der Merwe, P. A. Non-Catalytic Tyrosine-Phosphorylated Receptors. *Immunol. Rev.* **2012**, *250* (1), 258−276.
(43) Janeš, J. A.; Stumpf, H.; Schmidt, D.; Seifert, U.; Smith, A. S. Statistical Mechanics of an Elastically Pinned Membrane: Static Profile and Correlations. *Biophys. J.* **2019**, *116* (2), 283−295.
(44) Smith, A.-S.; Seifert, U. Vesicles as a Model for Controlled (de-)Adhesion of Cells: A Thermodynamic Approach. *Soft Matter* **2007**, *3*, 275.
(45) Janeš, J. A.; Monzel, C.; Schmidt, D.; Merkel, R.; Seifert, U.; Sengupta, K.; Smith, A.-S. First-Principle Coarse-Graining Framework for Scale-Free Bell-Like Association and Dissociation Rates in Thermal and Active Systems. *Phys. Rev. X* **2022**, *12*, 031030.
(46) Sherman, E.; Barr, V.; Samelson, L. E. Super-Resolution Characterization of TCR-Dependent Signaling Clusters. *Immunol. Rev.* **2013**, *251* (1), 21−35.
(47) Judokusumo, E.; Tabdanov, E.; Kumari, S.; Dustin, M. L.; Kam, L. C. Mechanosensing in T Lymphocyte Activation. *Biophys. J.* **2012**, *102*, L5−L7.
(48) O'Connor, R. S.; Hao, X.; Shen, K.; Bashour, K.; Akimova, T.; Hancock, W. W.; Kam, L. C.; Milone, M. C. Substrate Rigidity Regulates Human T Cell Activation and Proliferation. *J. Immunol. Baltim. Md 1950* **2012**, *189* (3), 1330−1339.
(49) Mordechay, L.; Le Saux, G.; Edri, A.; Hadad, U.; Porgador, A.; Schvartzman, M. Mechanical Regulation of the Cytotoxic Activity of Natural Killer Cells. *ACS Biomater. Sci. Eng.* **2021**, *7* (1), 122−132.
(50) Basu, R.; Whitlock, B. M.; Husson, J.; Le Floc'h, A.; Jin, W.; Oyler-Yaniv, A.; Dotiwala, F.; Giannone, G.; Hivroz, C.; Biais, N.; Lieberman, J.; Kam, L. C.; Huse, M. Cytotoxic T Cells Use Mechanical Force to Potentiate Target Cell Killing. *Cell* **2016**, *165* (1), 100−110.
(51) Aramesh, M.; Stoycheva, D.; Sandu, I.; Ihle, S. J.; Zünd, T.; Shiu, J.-Y.; Forró, C.; Asghari, M.; Bernero, M.; Lickert, S.; Kotowski, M.; Davis, S. J.; Oxenius, A.; Vogel, V.; Klotzsch, E. Nanoconfinement of Microvilli Alters Gene Expression and Boosts T Cell Activation. *Proc. Natl. Acad. Sci. U. S. A.* **2021**, *118* (40), No. e2107535118.
(52) Le Saux, G.; Bar-Hanin, N.; Edri, A.; Hadad, U.; Porgador, A.; Schvartzman, M. Nanoscale Mechanosensing of Natural Killer Cells Is Revealed by Antigen-Functionalized Nanowires. *Adv. Mater.* **2019**, *31* (4), No. 1805954.
(53) Bhingardive, V.; Le Saux, G.; Edri, A.; Porgador, A.; Schvartzman, M. Nanowire Based Guidance of the Morphology and Cytotoxic Activity of Natural Killer Cells. *Small* **2021**, *17* (14), No. 2007347.
(54) Rathar, R.; Sanchez-Fuentes, D.; Lachuer, H.; Meire, V.; Boulay, A.; Desgarceaux, R.; Blanchet, F. P.; Carretero-Genevrier, A.; Picas, L. Tuning the Immune Cell Response through Surface Nanotopography Engineering. *Small Sci.* **2024**, *4* (9), No. 2400227.
(55) Adutler-Lieber, S.; Zaretsky, I.; Platzman, I.; Deeg, J.; Friedman, N.; Spatz, J. P.; Geiger, B. Engineering of Synthetic Cellular Microenvironments: Implications for Immunity. *J. Autoimmun.* **2014**, *54*, 100.
(56) Cai, H.; Muller, J.; Depoil, D.; Mayya, V.; Sheetz, M. P.; Dustin, M. L.; Wind, S. J. Full Control of Ligand Positioning Reveals Spatial Thresholds for T Cell Receptor Triggering. *Nat. Nanotechnol.* **2018**, *13*, 610−617.
(57) Doh, J.; Irvine, D. J. Immunological Synapse Arrays: Patterned Protein Surfaces That Modulate Immunological Synapse Structure Formation in T Cells. *Proc. Natl. Acad. Sci. U. S. A.* **2006**, *103*, 5700−5705.
(58) Deeg, J.; Axmann, M.; Matic, J.; Liapis, A.; Depoil, D.; Afrose, J.; Curado, S.; Dustin, M. L.; Spatz, J. P. T Cell Activation Is Determined by the Number of Presented Antigens. *Nano Lett.* **2013**, *13* (11), 5619−5626.
(59) Keydar, Y.; Le Saux, G.; Pandey, A.; Avishay, E.; Bar-Hanin, N.; Esti, T.; Bhingardive, V.; Hadad, U.; Porgador, A.; Schvartzman, M. Natural Killer Cells' Immune Response Requires a Minimal Nanoscale Distribution of Activating Antigens. *Nanoscale* **2018**, *10* (30), 14651−14659.

https://doi.org/10.1021/acs.nanolett.5c02361
Nano Lett. 2025, 25, 11878−11887

(60) Schvartzman, M.; Wind, S. J. Robust Pattern Transfer of Nanoimprinted Features for Sub-5-Nm Fabrication. *Nano Lett.* **2009**, *9* (10), 3629−3634.
(61) Schvartzman, M.; Palma, M.; Sable, J.; Abramson, J.; Hu, X.; Sheetz, M. P.; Wind, S. J. Nanolithographic Control of the Spatial Organization of Cellular Adhesion Receptors at the Single-Molecule Level. *Nano Lett.* **2011**, *11* (3), 1306−1312.
(62) Cai, H.; Wolfenson, H.; Depoil, D.; Dustin, M. L.; Sheetz, M. P.; Wind, S. J. Molecular Occupancy of Nanodot Arrays. *ACS Nano* **2016**, *10* (4), 4173−4183.
(63) Zhang, D. K. Y.; Adu-Berchie, K.; Iyer, S.; Liu, Y.; Cieri, N.; Brockman, J. M.; Neuberg, D.; Wu, C. J.; Mooney, D. J. Enhancing CAR-T Cell Functionality in a Patient-Specific Manner. *Nat. Commun.* **2023**, *14* (1), 506.
(64) Yassin, A. A.-K.; Ureña Martin, C.; Le Saux, G.; Pandey, A.; Tzadka, S.; Toledo, E.; Pandit, J. J.; Sherf, T.; Nusbaum, I.; Bhattachrya, B.; Banerji, R.; Greenshpan, Y.; Abu Ahmad, M. A.; Radinsky, O.; Sklartz, M.; Gazit, R.; Elkabets, M.; Ghassemi, S.; Cohen, O.; Schvartzman, M.; Porgador, A. Mechanostimulatory Platform for Improved CAR T Cell Immunotherapy. *Adv. Mater.* **2025**, 2412482.

https://doi.org/10.1021/acs.nanolett.5c02361
Nano Lett. 2025, 25, 11878−11887